Methionine 129 variant of human prion protein oligomerizes more rapidly than the valine 129 variant - Implications for disease susceptibility to Creutzfeldt-Jakob disease

Title

Methionine 129 variant of human prion protein oligomerizes more rapidly than the valine 129 variant: implications for disease susceptibility to CJD

Authors

Abdessamad Tahiri-Alaoui[1], Andrew C. Gill[2], Petra Disterer[1] and William James[1]

Affiliations

[1]Sir William Dunn School of Pathology, University of Oxford, South Parks Road, Oxford OX1 3RE, UK. [2]Institute for Animal Health, Compton, Berkshire, Newbury, RG20 7NN, UK.

Corresponding author

Abdessamad Tahiri-Alaoui

email: abdou.tahiri-alaoui@path.ox.ac.uk

Telephone: (+44) 1865 275545

Fax: (+44) 1865 285756

The human PrP gene (*PRNP*) has two common alleles that encode either methionine or valine at codon 129. This polymorphism modulates disease susceptibility and phenotype of human transmissible spongiform encyphalopathies (TSEs) but the molecular mechanism by which these effects are mediated remains unclear. Here, we compared the misfolding pathway that leads to the formation of β-sheet-rich oligomeric isoforms of the methionine 129 variant of PrP to that of the valine 129 variant. We provide evidence for differences in the folding behaviour between the two variants at the early stages of oligomer formation. We show that Met129 has a higher propensity to form β-sheet-rich oligomers whereas Val129 has a higher tendency to fold into α-helical-rich monomers. An equimolar mixture of both variants displayed an intermidate folding behaviour. We show that the oligomers of both variants are initially a mixture of α-rich and β-rich conformers that evolve with time to an increasingly homogeneous β-rich form. This maturation process, which involves no further change in proteinase-K resistance, occurs more rapidly in the Met129 form than the Val129 form. Although the involvement of such β-rich oligomers in prion pathogenesis is speculative, the misfolding behaviour could, in part, explain the higher susceptibility of individuals that are methionine homozygote to both sporadic and variant CJD.

INTRODUCTION

The transmissible spongiform encephalopathies (TSEs) are a group of fatal, neurodegenerative disorders that affect humans and animals and are believed to be caused by a novel class of infectious pathogen, the prion (1,2). These diseases have attracted considerable interest not only because of their unique biology but also because of the appearance of new variant of Creutzfeldt-Jakob disease (vCJD) (3), which appears to be caused by dietary exposure to the causative agent of bovine spongiform encephalopathy (BSE) (4,5). At the heart of disease pathogenesis lies a poorly understood structural rearrangement of PrP, a host-encoded glycoprotein of the nervous and lymphoid systems. The normal cellular form of the prion protein (PrP^{C}) undergoes a conversion that leads to the accumulation of an abnormal, conformationally-altered isoform (PrP^{Sc}). According to the "protein-only" hypothesis of prion propagation, PrP^{Sc} is the principal or sole component of transmissible prions (6). PrP^{Sc} differs from PrP^{C} by increased β-sheet content, increased resistance to proteinase K and an oligomeric rather than a monomeric state (7).

The human PrP gene (*PRNP*) exists in two major allelic forms that encode either methionine or valine at codon 129, with allele frequencies of 0.63 and 0.37 in western European and American populations, respectively (8,9). This polymorphism is a key determinant of susceptibility to sporadic (10) and acquired (8,11) prion diseases and may affect age at onset (12-14). Based on the analysis of 300 sporadic CJD subjects, Parchi et al. identified six distinct clinicopathological variants of sCJD, which appeared to be specified largely by the genotype at codon 129 and the physiochemical properties of PrP^{Sc} (14). More recently, an extensive analysis, which included the metal ion-dependent conformation of PrP^{Sc}, of a large number of sCJD cases showed that PrP^{Sc} types are associated with the residue encoded at codon 129, the duration of illness and with neuropathological phenotype (15). PrP^{Sc} types 1 and 4 have so far been detected only in Met129 homozygotes, type 4 being uniquely associated with vCJD, type 3 in cases containing a Val129 allele and type 2 in any *PRNP* codon 129 genotype (16). The codon 129 polymorphism seemed to modulate the pattern of neuropathology and the extent of lesions in sCJD, as shown in a study that involved 70 patients who died in France between 1994 and 1998 (17). Codon 129 polymorphism also has epistatic effects on the phenotypic effects of mutations

elsewhere in the prion gene. For example, the Asp178Gln mutation combined with a methionine at position 129 results in fatal familial insomnia (FFI) (18). In contrast, the same mutation with a valine encoded at position 129 results in familial CJD (19). Similarly, Val129 homozygotes in association with the Phe198Ser mutation predispose patients to the Indiana kindred variant of Gerstmann-Straussler-Scheinker (GSS) disease (20). Furthermore, an increased prevalence of genotype Val/Val at the polymorphic site 129 has been described in patient with early onset Alzheimer's disease (21) and a shift in cognitive decline towards early age in carriers of *PRNP*129 Val/Val has recently been reported (22).

Despite the clear importance of the polymorphism at codon 129 in the *PRNP* gene and its link to disease susceptibility and pathogenesis, the molecular mechanisms by which these effects are mediated remain unclear. The *in vitro*, thermodynamic stability of recombinant PrP is not affected by the Met129Val mutation or by other substitutions related to inherited human prion diseases (23). Structural studies, however, have shown evidence for hydrogen bonding between residues 128 and 178, which might provide a structural basis for the highly specific influence of polymorphism in position 129 on disease phenotype that segregates with Asp178Gln (24). Molecular dynamic simulations of low pH-induced conformational conversion of PrP has provided further clues as to the role of residue 129 (25). In these simulations, Met129 seems to interact with Val122 leading to the recruitment of more N-proximal residues into an expanding β-sheet. As a complementary approach, we have chosen to study the folding properties of the two PrP allelomorphs experimentally, by examining the misfolding pathway that leads to the formation of β-sheet-rich oligomeric isoforms (26). We show that PrP-Met129 has a higher propensity to form β-sheet-rich oligomers whereas PrP-Val129 has a higher tendency to fold into α-helical-rich monomers. We also provide evidence that the dynamics of maturation of the oligomers differ between the two variants. The maturation process occurs over time at the expense of the α-helical-like monomers at a faster rate for PrP-Met129 than for PrP-Val129. Once the oligomers from either allelomorph have been formed they show similar proteinase K resistance that does not change throughout the oligomer maturation process. The observed differences in the

misfolding of PrP-Met129 and PrP-Val129 could explain the high susceptibility of individuals that are methionine homozygote to sporadic as well as variant CJD.

MATERIALS AND METHODS

Cloning of PrP genes and protein purification. Genomic DNA encoding methionine/valine at codon 129 of *PRNP* gene (18) was extracted from the blood of a heterozygote individual using standard phenol-chloroform methods. The fragment of the *PRNP* gene spanning codon 90 through 231 was amplified with the oligonucleotide primers 5′-cgggatcccatgcaaggaggtggcacccacagtcagtggaacaagccg-3′ and 5′-cccaagcttcatgctcgatcctctctggtaataggcctgag-3′ in 100 μl PCR buffer that contained 300 ng of each DNA, 2 units *Taq* DNA polymerase, 200 μM of each dNTP, 0.2 μM of each primer, 3.5 μM $MgCl_2$, 10 mM Tris-HCl pH 9.0, 0.1 % Triton X-100, 50 mM KCl. The following PCR conditions were used: an initial denaturation (95°C, 3 min) followed by 25 cycles of denaturation (95°C, 1 min), annealing (55°C, 1 min), extension (72°C, 1 min), and a final elongation (72 °C, 8 min). Restriction sites *Bam*HI and *Hin*dIII, including extra-nucleotides for efficient cleavage close to the ends, were introduced in the primers. The PCR fragment was cloned into the pTrcHis2B vector that incorporated a C-terminal His-tag (Invitrogen life technologies, Paisley, UK) according to the manufacturer's instructions. The identity of human PrP clones was confirmed by sequencing with the BigDye Terminator v3.0 on ABI-Prism 3100 Genetic Analyzer (Applied Biosystems). The clones corresponding to PrP^{90-231} with Met129 or Val129 were identified by comparison with human PrP clones available in the databases (Accession numbers: M13667, P04156). *Escherchia coli* expression and purification of recombinant human PrP was performed as previously described (27) except that the buffer used to solubilise inclusion bodies did not contain DTT. Stocks of highly purified proteins were stored in 6 M guanidine hydrochloride, 50 mM Tris-HCl pH 7.2.

Oligomer formation by HPLC-gel filtration and dialysis methods. Rapid refolding of proteins into oligomeric isoforms was carried out at concentrations of 10 mg/ml and 30 mg/ml. PrP- Met129 and PrP-Val129 were denatured in 6 M guanidine hydrochloride, 50 mM Tris-HCl pH 7.2 and were injected (100 μl) onto a size

exclusion chromatography (SEC) column (TSK®-Gel SWXL G3000 HPLC column, 7.8 x 300 mm, Phenomenex, Macclesfield, UK), equilibrated in 20 mM sodium acetate, 0.2 M NaCl, pH 3.7, 1 M urea and 0.02% sodium azide (26). This rapid oligomer formation on SEC-HPLC corresponded to time zero as opposed to time course analysis of oligomer formation during dialysis. This time course analysis of oligomer formation was carried out as follows: 1 ml of 6M guanidine-hydrochloride-denatured proteins (10 mg/ml or 30 mg/ml), was dialysed at room temperature against 2 litres of 20 mM sodium acetate, 0.2 M NaCl, pH 3.7, 2 M urea by use of a Slide-A-Lyser dialysis cassette (Perbio Science UK Ltd, Tattenhall, UK) of 10 kDa cut off. Aliquots were withdrawn, after carefully shaking the cassette to ensure homogeneity, after 30 min, 2, 4 and 24 hours and analyzed by SEC as described above. Protein peaks were manually collected for subsequent analysis. Circular dichroism was carried as previously described (28) to assess the secondary structure of the protein.

Analytical Reversed-phase HPLC. Protein fractions collected during SEC analysis were kept in SEC elution buffer at room temperature and analyzed after 2, 12, 30, 110, 140, 200 and 300 days by analytical reversed-phase (RP) HPLC (Sephasil C4, 5 μm, 4.6 x 250 mm) (Amersham Biosciences, Little Chalfont, UK). Proteins were eluted with a linear gradient of H_2O + 0.1% TFA to 95 % acetonitrile + 0.09% TFA over 25 minutes.

All HPLC separations were performed at room temperature with a flow rate of 1 ml/min by means of a Perkin-Elmer HPLC system composed of a Binary LC pump 250 and a Diode array detector 235C controlled by Total Chrome software version 6.2 (Perkin-Elmer, Seer Green, UK), through a PE Nelson 600 series link. The eluent was monitored by UV absorption at 280 nm.

Proteinase K digestion. Recombinant human PrP collected from SEC-HPLC was subjected to proteinase K digestion after 2, 12 and 140 days maturation of the oligomers. The solution was incubated at 37 °C with a ratio of 1: 24 PK to protein in 20 mM sodium acetate, 0.2 M NaCl, pH 5.5. Aliquots of the digests were taken after 15, 30 and 60 minutes and snap frozen for analysis by SDS-PAGE and mass spectrometry.

On line capillary HPLC nanospray mass spectrometry. Mass spectrometry was carried out on a Quattro II tandem quadrupole mass spectrometer (Micromass UK Ltd, Altrincham, UK) equipped with on-line capillary HPLC as detailed in (29). Briefly, the capillary HPLC was 180 μm i.d. and was packed with 3.5 μm Jupiter C18 resin (Phenomenex, Macclesfield, UK). A flow rate of 1 μl/min was used and proteins were eluted with a gradient from 0-70% solvent A to B, where solvent A was 95:5 water:acetonitrile with 0.05% trifluoroacetic acid and solvent B was 95:5 water:acetonitrile with 0.05% trifluoroacetic acid. The eluent was passed directly to the mass spectrometer which was operated in continuous flow nanospray mode. Full scan mass spectra (m/z 300-2100) were acquired every 5 seconds.

RESULTS

Characterization of recombinant human PrP-Met129 and PrP-Val129

Recombinant human prion protein variants, HuPrP$^{90\text{-}231}$ Met129 and HuPrP$^{90\text{-}231}$ Val129, were purified to homogeneity by immobilized-metal affinity chromatography (see supplementary figure 1) followed by RP-HPLC. Purified proteins were analysed by mass spectrometry to confirm purity and identity. Omitting DTT from the buffer used to solubilize the inclusion bodies and allowing disulfide bond to form in the oxidizing environment of the IMAC was found to yield a fully oxidized protein (see supplementary figure 1) that has characteristics of PrP^{C}, such as a monomeric state, high α-helical content and proteinase K sensitivity. All the studies presented in this paper were performed on proteins that included a C-terminal His-tag.

PrP-Met129 has an intrinsically higher propensity to oligomerize than PrP-Val129

To assess the effect of the codon 129 polymorphic residue on the formation of non-native isoforms, both protein variants were denatured in 6 M guanidine hydrochloride, 50 mM Tris-HCl pH 7.2, and allowed to fold under conditions favouring the formation of β-oligomer species (26). To dissect the *in vitro* folding pathway of prion protein misfolding we used size exclusion chromatography (SEC), dialysis and circular dichroism (CD). The denatured proteins (30 mg/ml) were injected onto a SEC column that had previously been equilibrated in 20 mM sodium acetate, 0.2 M NaCl, pH 3.7, 1 M urea and 0.02% sodium azide and eluted with the same buffer. The

elution profile of the Met129 variant shows two major peaks and one minor peak (Fig. 1*A*). Peak I (terminology as given by Baskakov et al (26)) eluted at 5.68 min and corresponded to high molecular weight aggregates (Fig. 1*A*). Peak II eluted at 6.54 min and corresponded to the oligomeric isoform while peak III, which eluted at 9.08 min, had a similar retention time to monomeric protein (Fig. 1*A*). The elution profile of Val129 variant shows the same three peaks but in different proportions, with peak II eluting as a shoulder to peak I (Fig. 1*B*). In order to mimic a heterozygote situation of an individual that carries both alleles we have analyzed the folding behaviour in a 1:1 mixture of Met129 and Val129 (Fig 1*C*). The elution profile of the equimolar mixture showed three peaks as seen before (Fig 1*C*). Integration of the peaks in figure 1A and 1B revealed that less than 2% of the Val129 variant had formed oligomers under these rapid refolding conditions (within the first 10 minutes of the SEC-elution) as compared to more than 70% in the case of Met129 (Fig. 1*D*). In addition, the percentage of monomeric population that was formed within 10 minutes was calculated to be about 66% for the Val129 variant but only 24% for the Met129 variant (Fig. 1*D*). Integration of the peaks in the equimolar mixture showed that the percentage of oligomeric form was reduced to about 44%, corresponding to approximately 30% reduction in the amount of oligomers as compared to the situation of the Met129 alone (Fig. 1*D*). Also the amount of the monomeric population in the mixture 1:1 increased by about 17% when compared to that of the Met129 alone (Fig. 1*D*). The monomeric forms of Met129 and Val129 variants yielded CD spectra with two minima at 208 nm and 222 nm, indicative of a predominantly α-helical conformation (data not shown). The CD spectra of protein from peak II of PrP-Met129 and peaks I and II of PrP-Val129 did not give clear information about the protein conformations, but suggested that these fractions were composed of a mixture of α-helical and β-sheet forms.

To investigate the formation and evolution of the oligomers that eluted in peak II in more detail, we used a slower dialysis method of refolding that allowed analysis at different times after initiation of the refolding. Two protein concentrations, 30 and 10 mg/ml, were analyzed in parallel. The composition of the dialysis buffer was the same as that used in SEC elution buffer, except that, to maximize the formation of oligomers, the urea concentration was increased to 2 M (28). After 30 minutes

refolding, and at 30 mg/ml, both allelomorphs adopted predominately oligomeric forms (peak II) with virtually no monomeric protein present (peak III); this elution profile did not change over the course of the experiment (Fig. 2*A*). Similar results where obtained with a mixture (1:1) of Met129 and Val129 (data not shown). The CD spectra of oligomers collected at 30 min and 1 h showed that the population was not dominated by β-sheet rich structures but contained some α-helical rich protein (*Fig. 2, C-D*). However, by four hours the CD spectra of the protein contained in peak II from both allelomorphs were typical of proteins possessing high amounts of β-sheet and the spectra remained constant thereafter.

In contrast, at 10 mg/ml (Fig. 2*B*) the kinetics of oligomerization of PrP-Met129 were significantly different from those of the PrP-Val129. The disappearance of aggregated proteins from peak (I) occurred more rapidly in the Met129 variant than in the Val129 variant, which suggests that, under oligomer-promoting conditions, the aggregated material from PrP-Met129 has a higher propensity to convert into oligomer than aggregated protein from PrP-Val129. To test this, we took aggregated proteins from peak (I) of PrP-Met129 and PP-Val129 from SEC at time zero and monitored their evolution over time by re-injecting them onto the same SEC. Time course comparison between the two allelomorphes clearly demonstrated the higher propensity of the Met129 variant to oligomerize than the Val129 variant (see supplementary figure 2). Virtually all aggregated PrP-Met129 converted into oligomeric isoforms over a period of 12 days, whereas a substantial amount of PrP-Val129 remained as aggregates. To investigate the behaviour of monomeric species in peak III under the same oligomeric-promoting conditions we compared the rate of oligomerization of the Met129 variant to that of the Val129 variant collected from SEC at time zero. Time course comparison between the two allelomorphs clearly revealed that monomeric Met129 has a higher propensity to oligomerize than monomeric Val129. This difference in oligomerization rates was apparent after two days of incubation at room temperature (see supplementary figure 2).

From these data we conclude that, under these conditions, the Met129 variant has an intrinsically higher propensity to form oligomer isoforms than the Val129. The high oligomerization propensity of the methionine variant becomes even more apparent

under the highest protein concentration and rapid refolding conditions. Since this is true for denatured, aggregated or natively-folded monomeric protein, the higher propensity of oligomerisation is clearly independent of the starting state of the protein.

The oligomers of both Met129 and Val129 variants are conformationally heterogeneous and show different kinetics of maturation

It has been shown that the oligomeric isoforms of mouse and Syrian hamster PrP are formed of populations of structurally heterogeneous proteins (26). RP-HPLC analysis showed that reduced forms of recombinant mouse PrP existed in multiple β-sheet rich isoforms with distinct retention times (30,31). Accordingly, we used RP-HPLC to investigate the effect of the residue encoded at codon 129 on the composition of the oligomer population that eluted from SEC in peak II. Aliquots of this fraction were incubated at room temperature in SEC elution buffer (20 mM sodium acetate, 0.2 M NaCl, pH 3.7, 1 M urea and 0.02% sodium azide) and analyzed at various times (Fig. 3). After two days incubation, the RP chromatogram of PrP-Met129 showed two peaks with distinct retention times (Fig. 3*A*), however for PrP-Val129 only one major peak was observed (Fig. 3*B*). A second peak could be seen only after 12 days incubation. The two peaks were designated (IIa) and (IIb), with shorter and longer retention times, respectively. In order to rule out the possibility that the two peaks represented unexpected modification to the proteins, we analysed them by mass spectrometry (Fig. 4). The deconvoluted mass spectra of PrP-Met129 IIa and PrP-Met129 IIb demonstrate that they represent proteins of the same molecular mass (Fig. 4, *A*-B). Similarly, the deconvoluted mass spectra of PrP-Val129 IIa and PrP-Val129 IIb showed that they also represented proteins with similar molecular masses (Fig. 4, *C*-*D*). From these analyses we infer that no covalent differences are evident and that the two peaks observed by RP-HPLC represent different conformations, with different amounts of hydrophobic residues exposed at the protein surface.

Two important observations can be clearly made from RP-C4 chromatograms. Firstly, the proportions of the two forms of PrP-Met129 and PrP-Val129 were different; the proportion of protein eluting in peak (IIa) was higher for PrP-Met129 after 12 days incubation (Fig. 3, *A* vs. *B*), while for PrP-Val129 there was more protein that eluted

in peak (IIb). Secondly, the proportions of the two peaks changed over time at different rates for Met129 and Val129 variants. In particular, the proportion of protein eluting in peak (IIb) decreased at a higher rate in the oligomer of PrP-Met129 (Fig. 3*A*) than in the oligomer of PrP-Val129 (Fig. 3*B*). The peak (IIb) of the oligomer from both allelomorphs seemed to have a retention time similar to that of the corresponding α-helical monomers. Because RP-HPLC uses differences in the hydrophobic properties to achieve separation between bio-molecules, it can be concluded that the protein population present in the highly retained peak (IIb) has more surface-exposed hydrophobic residues than the protein population present in peak IIa. Furthermore, the protein population present in peak (IIb) appears to undergo conversion to become recruited into the population that eluted in peak (IIa). Over time, this conversion seemed to occur much quicker with PrP-Met129 than with PrP-Val129 (Fig. 3, *A* vs. *B*).

Because of the long storage time of both allelomorphs in SEC elution buffer at room temperature, we have used mass spectrometry to assess the integrity of the samples (see supplementary figure 3). After 2 and 12 days of oligomerization, both allelomorphs had molecular masses that matched those predicted from the amino acid sequences. However, after 30 days of oligomerization, the deconvoluted mass spectra of both variants showed an additional species with a molecular mass that corresponded to the cleavage of the N-terminal two residues from the proteins (see supplementary figure 3). The two variants showed the same level of cleavage that increased over time to yield, 300 days later, proteins that were completely lacking two residues from the N-terminus (see supplementary figure 3). The cleavage occurred in the peptide bond linking an aspartyl residue to a prolyl residue (Fig. 5*F*). The lability of Asp-Pro bonds under acidic conditions has previously been reported (32) and provides a simple explanation for our observation. The cleavage occurred at the same rate for both Met129 and Val129 variants and at a region of the N-terminal that was PK sensitive (see below) and, therefore, was unlikely to impact the differences that were observed during oligomerization of the two allelomorphs.

The oligomers of Met129 and Val129 show similar proteinase K resistance

Limited PK digestion has been used widely to distinguish the disease isoform, PrP^{Sc}, from PrP^{C} as well as to probe differences between PrP^{Sc} strains (33,34). We therefore used limited PK digestion in combination with on-line capillary HPLC mass spectrometry to probe differences between Met129 and Val129 variants during oligomerization. After treatment for up to 60 min with a 1:24 ratio of PK to protein, capillary HPLC_MS demonstrated that digestion of the oligomers from both allelomorphs yielded a range of short peptides that eluted before 20 min (insets in Fig. 5, *A*-*B*) that were liberated from the N-terminal and C-terminal His-tag regions of the protein. The central and C-terminal domains remained intact and eluted after 20 min as two peaks from the reversed phase column (insets in Fig. 5, *A*-*B*). These polypeptides separated into two peaks that started either from residues 117 or 135 respectively, as a result of differential cleavage within the hydrophobic region (Fig. 5*F*). Comparison of deconvoluted mass spectra of polypeptides starting at 117 between PrP-Met129 (Fig. 5*A*) and PrP-Val129 (Fig. 5*B*) oligomers, showed three major PK-resistant cores with matching cleavage sites for each variant. The differences in masses (32 Da) between these PK-resistant fragments were due only to the presence of methionine or valine at position 129. Similarly, the comparison of deconvoluted mass spectra of polypeptides that started at 135 between PrP-Met129 (Fig. 5*C*) and PrP-Val129 (Fig. 5*D*) oligomers, revealed four major PK-resistant polypeptides with identical molecular masses for Met129 and Val129. Most, if not all, of the C-terminal His-tag remained PK-sensitive (Fig. 5*F*) during oligomerization, indicating that it was unlikely to interfere with the oligomerisation process. SDS-PAGE separation of the PK digests at various times of oligomerization (Fig. 5*E*) provided additional evidence that oligomers from PrP-Met129 and PrP-Val129 have similar PK-resistant properties.

DISCUSSION

In this work we show that the polymorphism at codon 129 affects the kinetics of oligomerization that leads to non-native isoforms of human prion protein. Starting from an unfolded state and when forced rapidly to adopt the oligomeric form under low pH and at high protein concentration, the Met129 variant clearly exhibited a preference for the oligomeric state, whereas Val129 variant favoured the α-helical-rich, monomeric state. We have ruled out the possibility that the denatured starting

protein contained any oligomeric forms of PrP by SEC analysis under denaturing conditions using 6M guanidine hydrochloride, 50 mM Tris-HCl pH 7.2 as elution buffer. Indeed the chromatograms showed only monomeric population of both PrP variants (see supplementary figure 4). How then does residue129 influence this folding behaviour? The first clue can be derived from the solution structure of human PrP determined by NMR (35). Residue 129 lies within the first β-strand (residues 128-131) in human PrP. Riek et al (36) proposed that this short β-sheet might be a 'nucleation site' for a conformational transition from PrP^{C} to PrP^{Sc} that could include the loops connecting the β-sheet to the first helix. Prion peptide models have also indicated the possible involvement of the region containing the first β-strand in the conformational switch of PrP (37,38).To our knowledge there is no published structure of Val129 variant of human PrP, however, molecular dynamic simulations of Syrian hamster PrP^{90-231} at neutral pH showed that when a valine residue was present at position 129 instead of a methionine residue, the proportion of protein with three-stranded, antiparallel β-sheet structure increased from 0% to 23% (39). The three β-strands spanned residues 115-116, 119-122 and 129-130 without affecting the thermodynamic stability of PrP, as was demonstrated experimentally (23). Molecular dynamic simulations of Syrian hamster $PrP^{109-219}$ at low pH revealed that regions around β-strand 1 and β-strand 2 were potential sites for conversion to β-structures (25). In particular, the first β-strand served as a structural nucleus for the formation of new, and propagation of existing, β-like structure (25). The interactions between Met129 and Val122 and between Tyr128 and Tyr162 illustrated the role of tertiary interactions between side chains nucleating secondary structure formation, as has been observed for helix formation in barnase (40).

Our experimental data show that, under conditions that favour rapid formation of oligomers, SEC can be used to partition protein folded into aggregated, monomeric and oligomeric states so that differences in folding of Met129 and Val129 variants become clear. It has been shown that folding of recombinant, murine prion protein into α-helix rich conformation is extremely rapid (41) and is under kinetic control (28). We show in this work that the propensity of recombinant human prion protein to fold into monomeric α-helical-rich population is increased when residue 129 was occupied by a valine. However, when the same position is occupied by methionine a

tendency for oligomerization can be observed, with comparatively little monomeric α-helical-rich population. These differences in folding behaviour can be explained by a fundamental event in protein folding, which is driven by a small number of specific residues involved in the formation of a well-defined, specific nucleus that then allows the rest of the structure to coalesce efficiently around it (42,43). The high β-sheet propensity of valine residues as compared to methionine residues (44,45) makes PrP in which valine is present at residue 129 more favourable to adopt the native local β-sheet that would temporarily stabilize the Val129 allelomorph in the monomeric α-helical PrP.

Differences between the oligomers formed from Met129 and Val129 could be seen when we explored the hydrophobicity of the oligomers as they evolved over time. These differences were consistent with early events that were observed during the rapid misfolding process. That is, the proportion of oligomer subunits with hydrophobic properties resembling those of the α-monomer was higher in PrP-Val129 than in the PrP-Met129. Over the course of several weeks of incubation, the oligomerization process in both variants occurred at the expense of the α-helical-like population that became a substrate for oligomer recruitment (28,46). The presence of the α-helical-like species in the oligomer reflected the heterogeneous nature of this non-native form of PrP. This finding was consistent with the previously published supra molecular electrospray ionisation mass spectrometry results (26). On the basis of these observations we propose a model (Fig. 6) that depicts the formation of non-native β-oligomers *in vitro*. Under appropriate conditions (low pH and high protein concentration) the acquisition of this non-native form can happen from either denatured, aggregated or native forms and involves two steps: a rapid oligomerization phase followed by a slow maturation phase characterized by a structural rearrangement of the oligomers. The presence of a methionine at codon 129 affects both the kinetics of oligomerization and those of the maturation phase.

A hallmark of the disease isoform, PrP^{Sc}, is its partial resistance to proteinase K digestion compared to normal cellular PrP. This property has also been used to probe differences between PrP^{Sc} conformations. We found that once oligomers from both allelomorphs are formed they show similar proteinase K resistance that does not

change throughout the oligomer maturation process. This indicates that if one relies solely on PK digestion to investigate PrP conformations, one could miss the detection of dynamic conformational changes influenced by the polymorphism at codon 129 in human PrP during disease pathogenesis.

It has been reported that two mutations in α-synuclein that are linked to early-onset Parkinson's disease can accelerate the oligomerization but not fibrilization suggesting that formation of nonfibrillar oligomer is likely to be critical in disease pathogenesis (47). There is no evidence so far that these β-oligomers exist *in vivo* or can directly cause prion diseases either alone or with the help of other factors. The high affinity and newly reported ligands that we have isolated in our laboratory (48,49) would help investigating the presence *in vivo* of the β-oligomers. The observed differences in the misfolding behaviour between Met129 and Val129 variants could provide a kinetic explanation to the observed high susceptibility of individuals that are methionine homozygote to sporadic as well as to variant CJD. Attempt to model a heterozygote situation by mixing Met129/Val129 (1:1) and allowing the rapid refolding to occur has yielded some promising results in that the amount of oligomers formed was reduced by approximately 30% as compared to the homozoygote-like situation in the Met129 alone, indicating certain degree of inhibition of the oligomerization in the heterozygote.

Phylogenetically, methionine is the ancestral amino acid at codon 129 (50), and Val129 is a mutation found in humans. Worldwide *PRNP* haplotype diversity and coding allele frequencies suggest that strong balancing selection at this locus occurred during the evolution of modern human and made heterozygosity at *PRNP* a significant selective advantage (51). Our data could provide a mechanism based on prion protein folding properties as an additional selective pressure against, particularly, Met129 homozygosity.

Acknowledments

AT-A is a University Research Lecturer supported by the Biotechnology and Biological Reseach Council, UK. WJ is a Fellow of Brasenose College, Oxford. AT-A, ACG and WJ wish to acknowledge the financial support of the BBSRC.

References

1. Prusiner, S. B. (1996) *Trends Biochem Sci* **21**, 482-487
2. Weissmann, C. (1996) *FEBS Lett* **389**, 3-11
3. Will, R. G., Ironside, J. W., Zeidler, M., Cousens, S. N., Estibeiro, K., Alperovitch, A., Poser, S., Pocchiari, M., Hofman, A., and Smith, P. G. (1996) *Lancet* **347**, 921-925
4. Bruce, M. E., Will, R. G., Ironside, J. W., McConnell, I., Drummond, D., Suttie, A., McCardle, L., Chree, A., Hope, J., Birkett, C., Cousens, S., Fraser, H., and Bostock, C. J. (1997) *Nature* **389**, 498-501
5. Hill, A. F., Desbruslais, M., Joiner, S., Sidle, K. C., Gowland, I., Collinge, J., Doey, L. J., and Lantos, P. (1997) *Nature* **389**, 448-450, 526
6. Prusiner, S. B. (1991) *Science* **252**, 1515-1522
7. Prusiner, S. B. (1998) *Proc Natl Acad Sci U S A* **95**, 13363-13383
8. Collinge, J., Palmer, M. S., and Dryden, A. J. (1991) *Lancet* **337**, 1441-1442
9. Windl, O., Dempster, M., Estibeiro, J. P., Lathe, R., de Silva, R., Esmonde, T., Will, R., Springbett, A., Campbell, T. A., Sidle, K. C., Palmer, M. S., and Collinge, J. (1996) *Hum Genet* **98**, 259-264
10. Palmer, M. S., Dryden, A. J., Hughes, J. T., and Collinge, J. (1991) *Nature* **352**, 340-342
11. Brown, P., Cervenakova, L., Goldfarb, L. G., McCombie, W. R., Rubenstein, R., Will, R. G., Pocchiari, M., Martinez-Lage, J. F., Scalici, C., Masullo, C., and et al. (1994) *Neurology* **44**, 291-293
12. Baker, H. E., Poulter, M., Crow, T. J., Frith, C. D., Lofthouse, R., and Ridley, R. M. (1991) *Lancet* **337**, 1286
13. Cervenakova, L., Goldfarb, L. G., Garruto, R., Lee, H. S., Gajdusek, D. C., and Brown, P. (1998) *Proc Natl Acad Sci U S A* **95**, 13239-13241
14. Parchi, P., Giese, A., Capellari, S., Brown, P., Schulz-Schaeffer, W., Windl, O., Zerr, I., Budka, H., Kopp, N., Piccardo, P., Poser, S., Rojiani, A., Streichemberger, N., Julien, J., Vital, C., Ghetti, B., Gambetti, P., and Kretzschmar, H. (1999) *Ann Neurol* **46**, 224-233
15. Hill, A. F., Joiner, S., Wadsworth, J. D., Sidle, K. C., Bell, J. E., Budka, H., Ironside, J. W., and Collinge, J. (2003) *Brain* **126**, 1333-1346
16. Collinge, J., Sidle, K. C., Meads, J., Ironside, J., and Hill, A. F. (1996) *Nature* **383**, 685-690
17. Hauw, J. J., Sazdovitch, V., Laplanche, J. L., Peoc'h, K., Kopp, N., Kemeny, J., Privat, N., Delasnerie-Laupretre, N., Brandel, J. P., Deslys, J. P., Dormont, D., and Alperovitch, A. (2000) *Neurology* **54**, 1641-1646
18. Goldfarb, L. G., Petersen, R. B., Tabaton, M., Brown, P., LeBlanc, A. C., Montagna, P., Cortelli, P., Julien, J., Vital, C., Pendelbury, W. W., and et al. (1992) *Science* **258**, 806-808
19. Goldfarb, L. G., Haltia, M., Brown, P., Nieto, A., Kovanen, J., McCombie, W. R., Trapp, S., and Gajdusek, D. C. (1991) *Lancet* **337**, 425
20. Dlouhy, S. R., Hsiao, K., Farlow, M. R., Foroud, T., Conneally, P. M., Johnson, P., Prusiner, S. B., Hodes, M. E., and Ghetti, B. (1992) *Nat Genet* **1**, 64-67

21. Dermaut, B., Croes, E. A., Rademakers, R., Van den Broeck, M., Cruts, M., Hofman, A., van Duijn, C. M., and Van Broeckhoven, C. (2003) *Ann Neurol* **53**, 409-412
22. Croes, E. A., Dermaut, B., Houwing-Duistermaat, J. J., Van den Broeck, M., Cruts, M., Breteler, M. M., Hofman, A., van Broeckhoven, C., and van Duijn, C. M. (2003) *Ann Neurol* **54**, 275-276
23. Liemann, S., and Glockshuber, R. (1999) *Biochemistry* **38**, 3258-3267
24. Riek, R., Wider, G., Billeter, M., Hornemann, S., Glockshuber, R., and Wuthrich, K. (1998) *Proc Natl Acad Sci U S A* **95**, 11667-11672
25. Alonso, D. O., DeArmond, S. J., Cohen, F. E., and Daggett, V. (2001) *Proc Natl Acad Sci U S A* **98**, 2985-2989
26. Baskakov, I. V., Legname, G., Baldwin, M. A., Prusiner, S. B., and Cohen, F. E. (2002) *J Biol Chem* **277**, 21140-21148
27. Jackson, G. S., Hill, A. F., Joseph, C., Hosszu, L., Power, A., Waltho, J. P., Clarke, A. R., and Collinge, J. (1999) *Biochim Biophys Acta* **1431**, 1-13
28. Baskakov, I. V., Legname, G., Prusiner, S. B., and Cohen, F. E. (2001) *J Biol Chem* **276**, 19687-19690
29. Gill, A. C., Ritchie, M. A., Hunt, L. G., Steane, S. E., Davies, K. G., Bocking, S. P., Rhie, A. G., Bennett, A. D., and Hope, J. (2000) *Embo J* **19**, 5324-5331
30. Lu, B. Y., Beck, P. J., and Chang, J. Y. (2001) *Eur J Biochem* **268**, 3767-3773
31. Lu, B. Y., and Chang, J. Y. (2001) *Biochemistry* **40**, 13390-13396
32. Landon. (1977) *Methods Enzymol* **47**, 145-149
33. Safar, J., Wille, H., Itri, V., Groth, D., Serban, H., Torchia, M., Cohen, F. E., and Prusiner, S. B. (1998) *Nat Med* **4**, 1157-1165
34. Bessen, R. A., and Marsh, R. F. (1994) *J Virol* **68**, 7859-7868
35. Zahn, R., Liu, A., Luhrs, T., Riek, R., von Schroetter, C., Lopez Garcia, F., Billeter, M., Calzolai, L., Wider, G., and Wuthrich, K. (2000) *Proc Natl Acad Sci U S A* **97**, 145-150
36. Riek, R., Hornemann, S., Wider, G., Billeter, M., Glockshuber, R., and Wuthrich, K. (1996) *Nature* **382**, 180-182
37. Nguyen, J., Baldwin, M. A., Cohen, F. E., and Prusiner, S. B. (1995) *Biochemistry* **34**, 4186-4192
38. Tahiri-Alaoui, A., Bouchard, M., Zurdo, J., and James, W. (2003) *Protein Sci* **12**, 600-608
39. Santini, S., Claude, J. B., Audic, S., and Derreumaux, P. (2003) *Proteins* **51**, 258-265
40. Wong, K. B., Clarke, J., Bond, C. J., Neira, J. L., Freund, S. M., Fersht, A. R., and Daggett, V. (2000) *J Mol Biol* **296**, 1257-1282
41. Wildegger, G., Liemann, S., and Glockshuber, R. (1999) *Nat Struct Biol* **6**, 550-553
42. Matouschek, A., Kellis, J. T., Jr., Serrano, L., and Fersht, A. R. (1989) *Nature* **340**, 122-126
43. Vendruscolo, M., Paci, E., Dobson, C. M., and Karplus, M. (2001) *Nature* **409**, 641-645
44. Kim, C. A., and Berg, J. M. (1993) *Nature* **362**, 267-270
45. Fasman, G. D. (1989) *Trends Biochem Sci* **14**, 295-299
46. Baskakov, I. V., Aagaard, C., Mehlhorn, I., Wille, H., Groth, D., Baldwin, M. A., Prusiner, S. B., and Cohen, F. E. (2000) *Biochemistry* **39**, 2792-2804
47. Conway, K. A., Lee, S. J., Rochet, J. C., Ding, T. T., Williamson, R. E., and Lansbury, P. T., Jr. (2000) *Proc Natl Acad Sci U S A* **97**, 571-576

48. Sayer, N. M., Cubin, M., Rhie, A., Bullock, M., Tahiri-Alaoui, A., and James, W. (2004) *J Biol Chem*
49. Rhie, A., Kirby, L., Sayer, N., Wellesley, R., Disterer, P., Sylvester, I., Gill, A., Hope, J., James, W., and Tahiri-Alaoui, A. (2003) *J Biol Chem* **278**, 39697-39705
50. Schatzl, H. M., Da Costa, M., Taylor, L., Cohen, F. E., and Prusiner, S. B. (1995) *J Mol Biol* **245**, 362-374
51. Mead, S., Stumpf, M. P., Whitfield, J., Beck, J. A., Poulter, M., Campbell, T., Uphill, J. B., Goldstein, D., Alpers, M., Fisher, E. M., and Collinge, J. (2003) *Science* **300**, 640-643

Figure legends

Fig. 1. Rapid refolding of recHuPrP$^{90-231}$ with C-terminal His-tag from denatured/unfolded state by SEC-HPLC under conditions that favoured oligomers formation. (**A**) recHuPrP$^{90-231}$ Met129, (**B**) recHuPrP$^{90-231}$ Val129 and (**C**) an equimolar mixture (1:1) of Met129 and Val129 in 6 M guanidine hydrochloride, 50 mM Tris-HCl pH 7.2 at 30 mg/ml were injected onto SEC and eluted with the equilibration buffer (20 mM sodium acetate, 0.2 M NaCl pH 3.7, 1 M urea and 0.02 % sodium azide). (**D**) The areas under the peaks were analyzed using Total Chrome software 6.2 and the data used to construct the plot allowing a direct comparison of the proportions of the peaks eluted from SEC between Met129 and Val129 variants.

Fig. 2. SEC profiles of fractions of recHuPrP$^{90-231}$ during time course refolding into oligomer isoforms using dialysis method. (**A**) and (**B**) are chromatograms of recHuPrP$^{90-231}$ Met129 and Val129 at 30 mg/ml and 10 mg/ml, respectively. Proteins in 6 M guanidine hydrochloride, 50 mM Tris-HCl pH 7.2 were dialyzed against 20 mM sodium acetate, 0.2 M NaCl pH 3.7, 2 M urea and aliquots were withdrawn from the dialysis cassette at the indicated time then injected onto SEC previously equilibrated in 20 mM sodium acetate, 0.2 M NaCl pH 3.7, 1 M urea, 0.02% sodium azide. (**C**) and (**D**) are CD spectra of Met129 and Val129, respectively, recorded at the indicated times after manual collection of the oligomer fraction that eluted in peak (II) from samples in panel (**A**).

Fig. 3. Time course analysis by RP-HPLC of oligomeric recHuPrP$^{90-231}$. Aliquots of (**A**) recHuPrP$^{90-231}$ Met129 and (**B**) recHuPrP$^{90-231}$ Val129 that were refolded by dialysis into oligomer isoforms for 4 hours then fractionated by SEC (see panel A, Fig. 2) were incubated at room temperature in SEC elution buffer (20 mM sodium acetate, 0.2 M NaCl pH 3.7, 1 M urea, 0.02% sodium azide) and anlalyzed by RP-C4 at the indicated times. The elution was done with a linear gradient of H_2O + 0.1% TFA to 95 % acetonitrile + 0.09% TFA over 25 minutes. For direct comparison of retention times, monomeric α-helical and denatured (6M guanidine hydrochloride) PrPs were analyzed by RP-HPLC under the same conditions.

Fig. 4. Nanospray mass spectrometry analysis of peaks IIa and IIb after 12 days of oligomerization. Peak IIa and IIb that were resolved by HPLC-RPC4 during the oligomerization of Met129 and Val129 were manually collected and immediately subjected to mass spectrometry analysis. (A) and (B) are electrospray mass spectra and deconvoluted (see insets) mass spectra of peaks IIa and IIb, respectively, of Met129 oligomer. (C) and (D) are electrospray mass spectra and deconvoluted (see insets) mass spectra of peaks IIa and IIb, respectively, of Val129 oligomer.

Fig. 5. Nanospray mass spectrometry and SDS-PAGE analysis of the proteinase K digests from oligomeric recHuPrP$^{90-231}$. (**A**) Deconvoluted mass spectrum of polypeptides eluting at 23.35 minutes from C-18 reversed phase capillary HPLC (see inset) of Met129 oligomers. These correspond to residues 117-225 (12678 Da), 117-232 (13488 Da) and 117-244 (14840 Da). (**B**) Deconvoluted mass spectrum of polypeptides eluting at 22.90 minutes (see inset) of Val129 oligomers. These correspond to residues 117-225 (12 646 Da), 117-232 (13456 Da) and 117-244 (14808 Da). (**C**) Deconvoluted mass spectrum of polypeptides eluting at 21.33 minutes (see inset in panel **A**) of Met129 oligomers. These correspond to residues 135-222 (10752 Da), 135-225 (11114 Da), 135-232 (11924 Da) and 135-244 (13276). (**D**) Deconvoluted mass spectrum of polypeptides eluted at 21.55 minutes (see inset in panel B) of Val129 oligomers. These correspond to residues 135-222 (10752 Da), 135-225 (11114 Da), 135-232 (11924 Da) and 135-244 (13276 Da). (**E**) Coomassie-stained SDS-PAGE of limited proteinase K digests from Met129 and Val129 after 2, 12 and 140 days of oligomerization. The digestion was carried out at 37 °C at the indicated incubation times with a ratio 1:24 PK to protein. (**F**) The PK-resistant fragments that were identified by mass spectrometry are overlaid on the amino acid sequence of human PrP Met/Val129. The residues that were introduced into the recombinant HuPrP for cloning and purification purposes are indicated in green at the N-terminal and in blue at the C-terminal.

Fig. 6. Schematic model illustrating *in vitro* formation and maturation of oligomer isoforms of recHuPrP$^{90-231}$ Met129 and Val129. Under appropriate conditions (low pH and high protein concentration) the acquisition of non-native form can happen from either denatured, aggregated or native forms and involves two steps: a rapid oligomerization phase followed by a slow maturation phase characterized by a

structural rearrangement of the oligomers. The presence of a methionine at codon 129 affects both the kinetics of oligomerization and those of the maturation phase.

Figure legends
(Supporting information)

Fig. 1. Characterization and purification of allelomorphs of cloned Human PrP^{90-231} with C-terminal His-tag. (**A**) and (**B**) are regions of the ABI traces showing the polymorphism at codon 129 in methionine and valine variants of PrP, respectively. (**C**) Representative chromatogram showing the elution profile of recHuPrP (Met129) during Ni-NTA sepharose-FPLC purification. (**D**) Coomassie-blue stained 18% SDS-PAGE of selected fractions illustrating the level of purity of recHuPrP achieved from the metal affinity purification. (**E**) Characterization of the redox state of both allelomorphs of recHuman PrP^{90-231} with C-terminal His-tag by reversed-phase HPLC. Aliquots from the pooled fractions P3 (see panel **C**) were run on analytical RP-C4 HPLC either before or after treatment with 100 mM DTT. One concludes from the retention time that both variants were fully oxidized after Ni-NTA sepharose-FPLC purification. After treatment with DTT both proteins became reduced and opened therefore exposing more hydrophobic residues to interact with the C4-alkyl chain hence requiring higher percentage of organic solvent for their elution which resulted in a higher retention times.

Fig. 2. Time course analysis of the aggregated and monomeric fractions from Met129 and Val129 under oligomer promoting condtions by SEC and PK digestion. (**A**) and (**B**) are chromatograms showing comparative evolution between Met129 and Val129, respectively, of aggregated fractions. Similarly, (**C**) and (**D**) are chromatograms showing comparative evolution between Met129 and Val129, respectively, of monomeric fractions. The protein concentration in each fraction was adjusted to 1 mg/ml and incubated in SEC elution buffer (20 mM sodium acetate, 0.2 M NaCl pH 3.7, 1 M urea, 0.02% sodium azide) at room temperature. Frations of 100 µl were injected onto SEC at the indicated times. (**E**) and (**F**) are coomassie-stained SDS-PAGE of proteinase K digests from Met129 and Val129 after 0.04 (1 hour), 6 and 30 days of oligomerization. The digestion was carried out at 37 °C at the indicated incubation times with a ratio of 1:24 (PK to protein).

Fig. 3. Electrospray mass spectra and deconvoluted mass spectra of Met129 and Val129 allelomorphs over time during oligomerization. Because of the long storage

time of both allelomorphs in size exclution chromatography elution buffer (20 mM sodium acetate, 0.2 M NaCl, pH 3.7, 1 M urea and 0.02% sodium azide) at room temperature, we have used mass spectrometry to assess the integrity of the samples. After 2 days of oligomerization, both allelomorphs had molecular masses that matched the theoretical ones. However, after 30 days of oligomerization the deconvoluted mass spectra of both variants showed an additional species with a molecular mass that corresponded to the cleavage of two residues from the N-terminal part of the proteins. The two allelomorphs showed the same level of cleavage that seemed to continue over time to yield, 300 days later, proteins that were completely lacking two residues from the N-terminus. The amino acid sequence of cloned human PrP showed that the cleavage occurred in the peptide bond linking aspartyl residue to prolyl residue. The lability of Asp-Pro bonds has been reported before and therefore provides a simple explanation for our observation in the context of acidic conditions used during the oligomerization. The observed cleavage occurred at the same rate and equally between Met129 and Val129 and at a region of the N-terminal that was PK sensitive, therefore it was unlikely to impact the observed oligomerization differences

Fig. 4. Overlay of SEC profiles of methionine 129 and valine 129 of recHuPrP$^{90\text{-}231}$ under mild (1 M urea) and strong denaturing (6 M guanidine hydrochloride) conditions. (**A**) Met129 and Val129 PrP in 6 M guanidine hydrochloride, 50 mM Tris-HCl pH 7.2 at 30 mg/ml were injected onto SEC previously equilibrated in 20 mM sodium acetate, 0.2 M NaCl pH 5.5, 1 M urea and 0.02 % sodium azide, then eluted with the same buffer (B) Met129 and Val129 PrP in 6 M guanidine hydrochloride, 50 mM Tris-HCl pH 7.2 at 30 mg/ml were injected onto SEC previously equilibrated in 6 M guanidine hydrochloride, 50 mM Tris-HCl pH 7.2, then eluted with the same buffer. The injected volumes were 100 µl. Under both conditions the chromatograms revealed the presence of only monomeric species that eluted approximately at 9 minutes, thus excluding the possibility of the pre-existing oligomeric specices in 6 M guanidine hydrochloride, 50 mM Tris-HCl pH 7.2 buffer.

Figure 1
Tahiri-Alaoui et al.

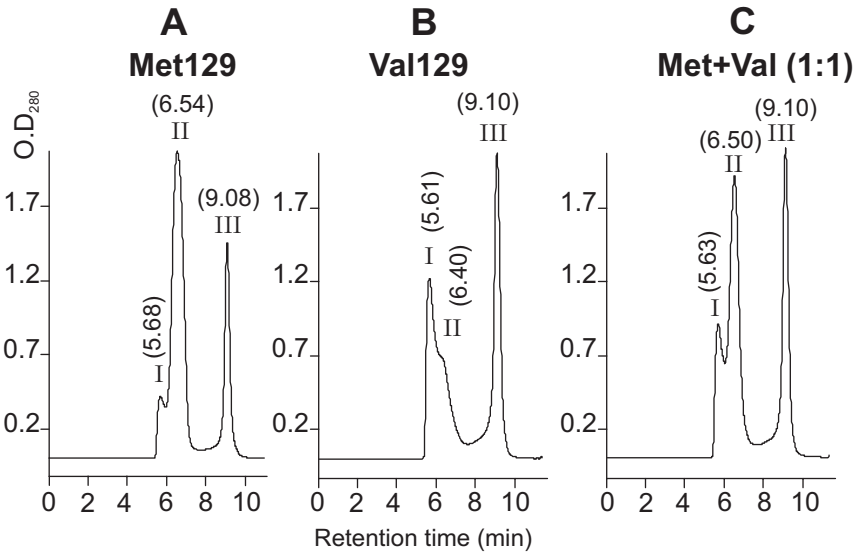

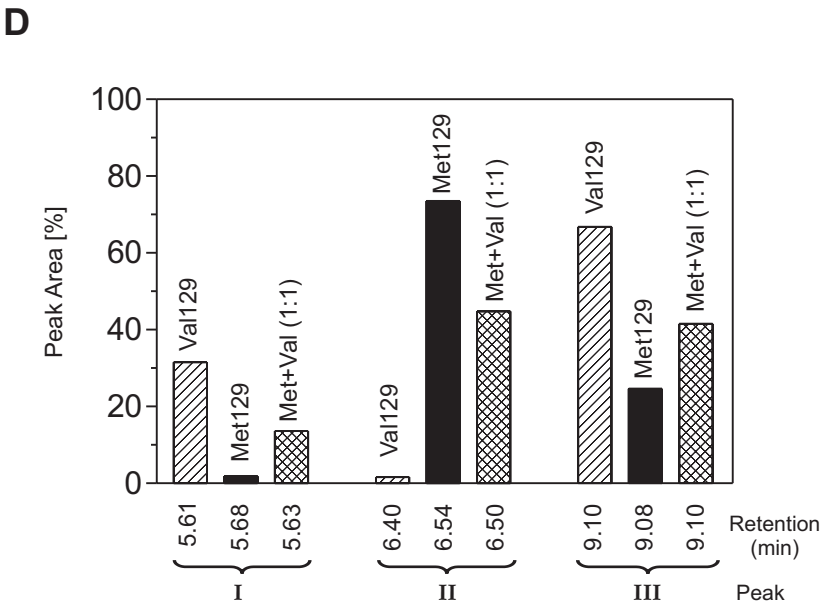

Figure 2
Tahiri-Alaoui et al.

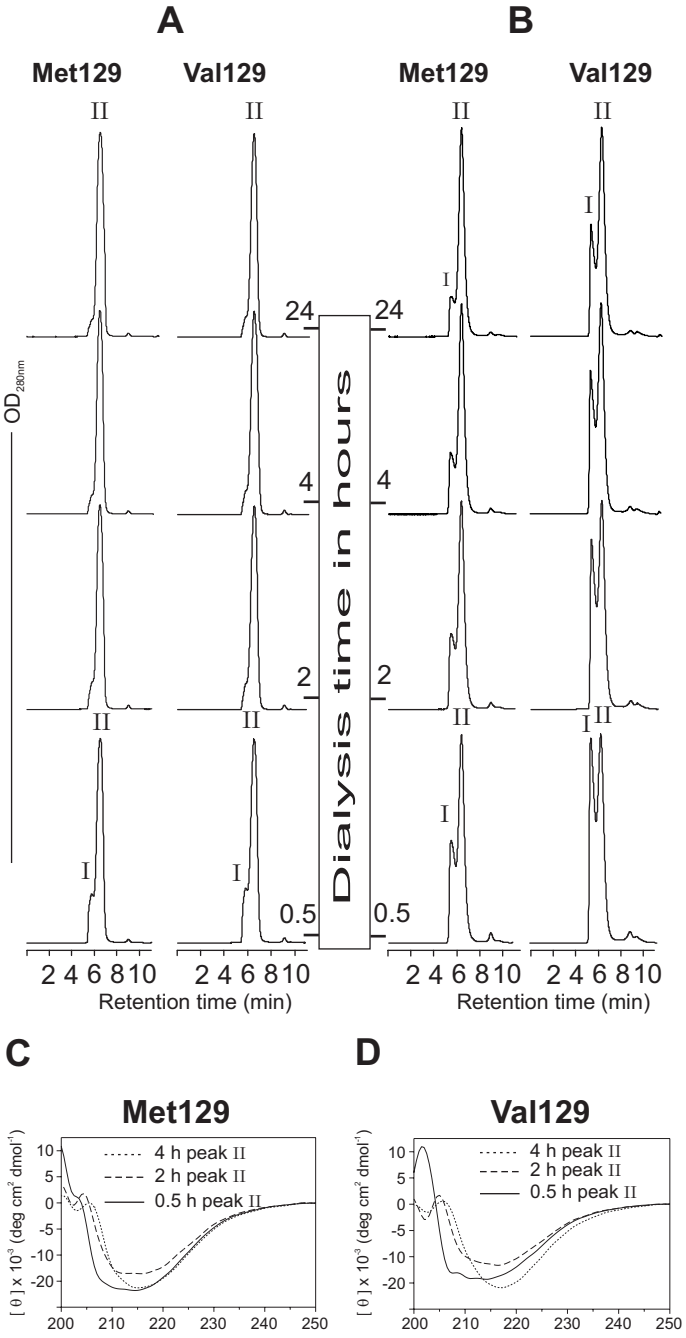

Figure 3
Tahiri-Alaoui et al.

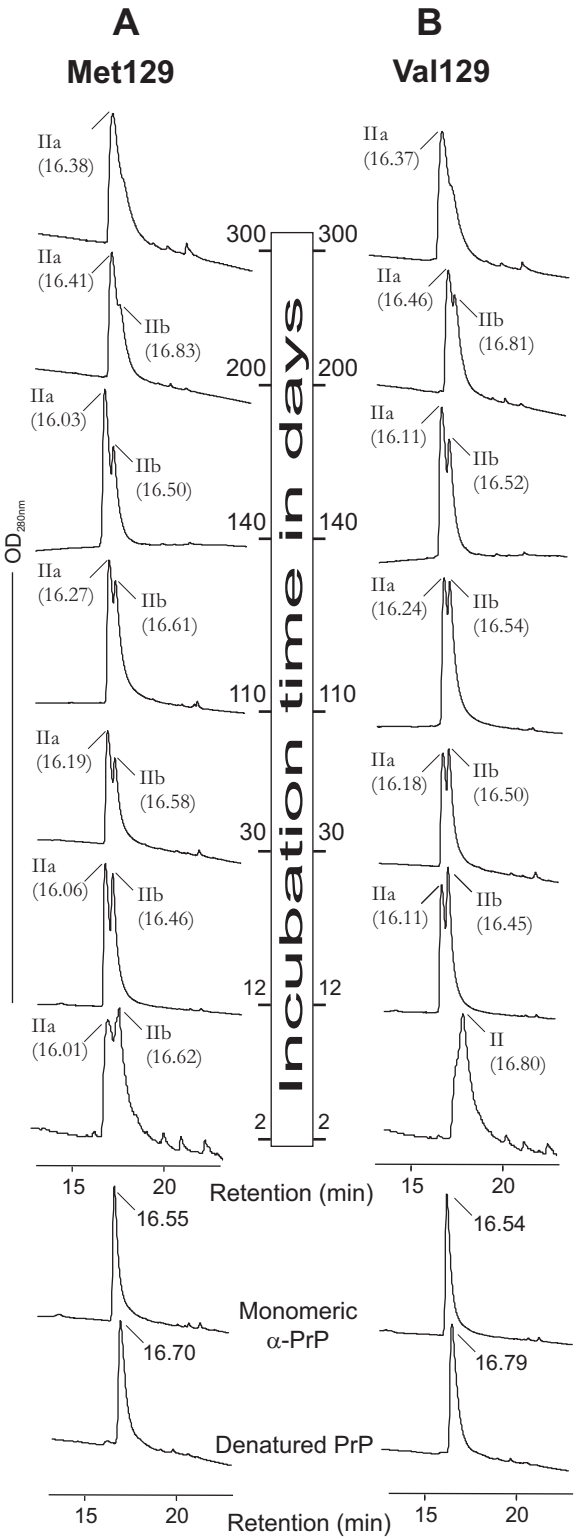

Figure 4
Tahiri-Alaoui et al.

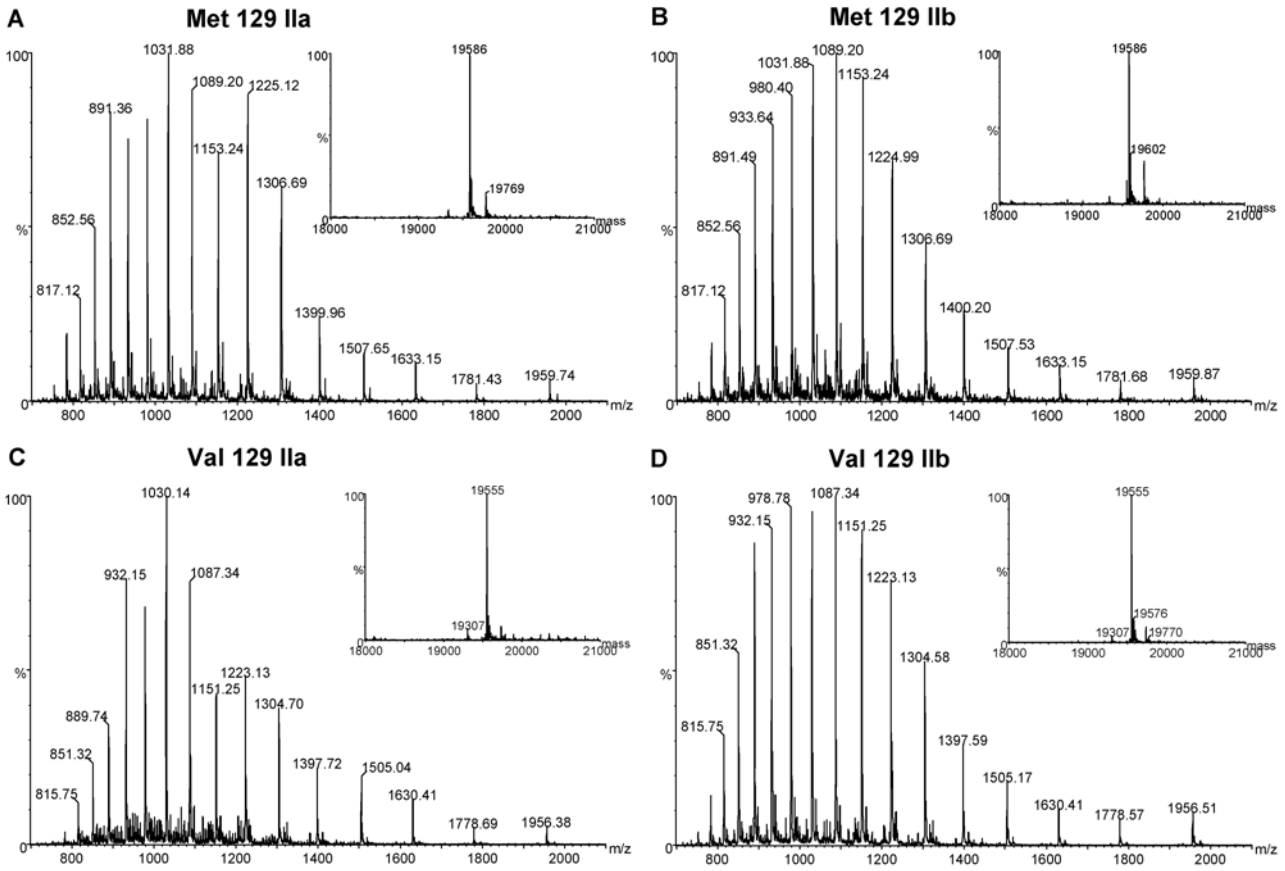

Figure 5
Tahiri-Alaoui et al.

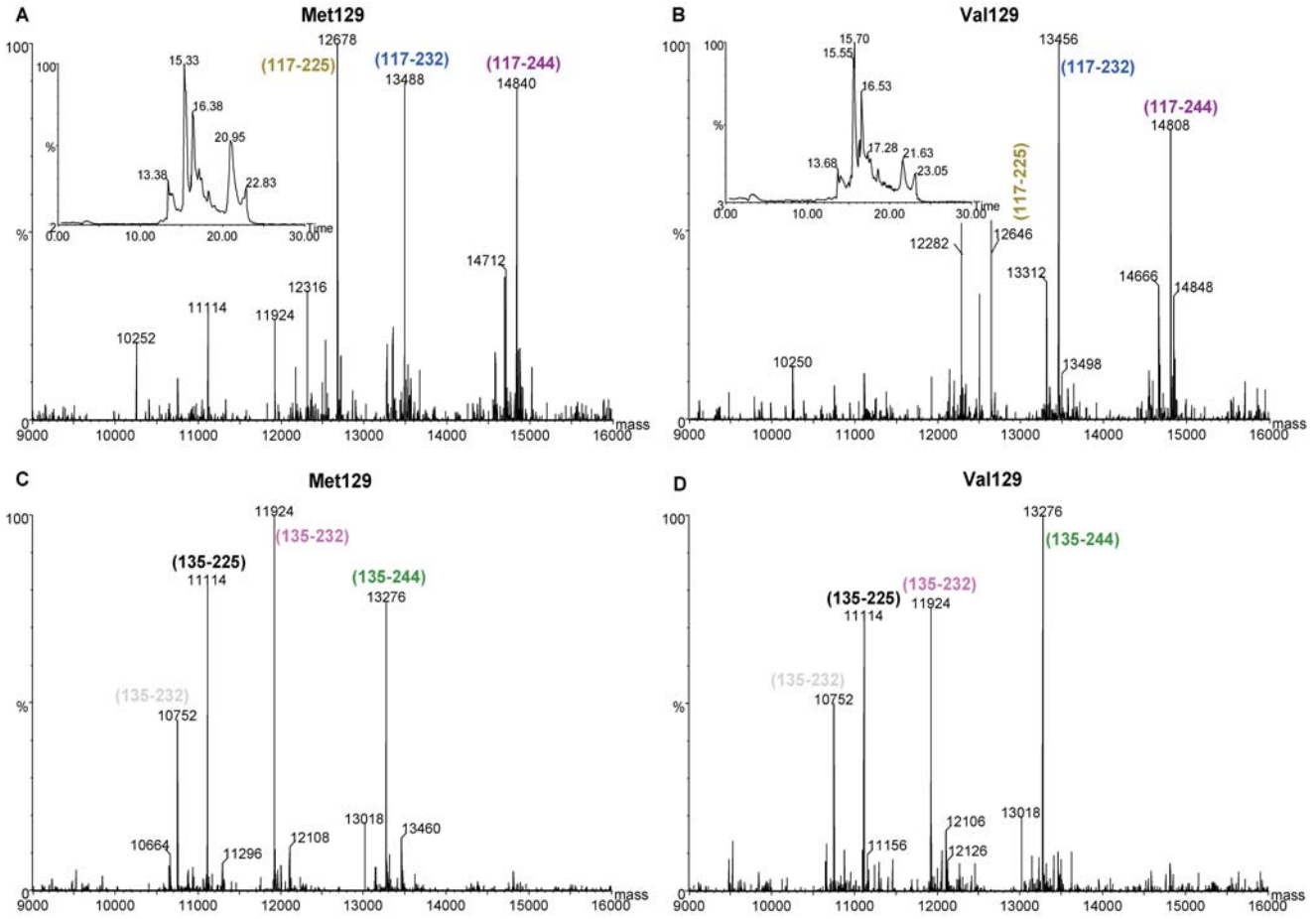

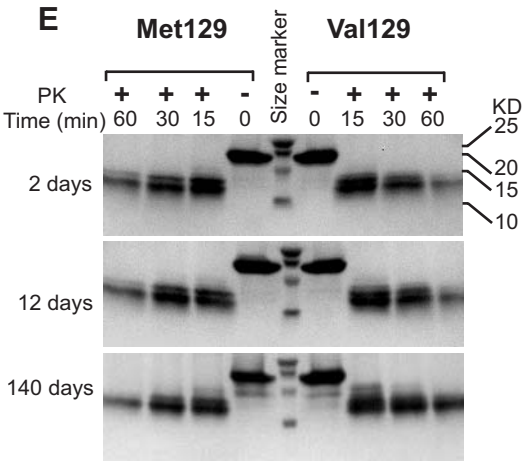

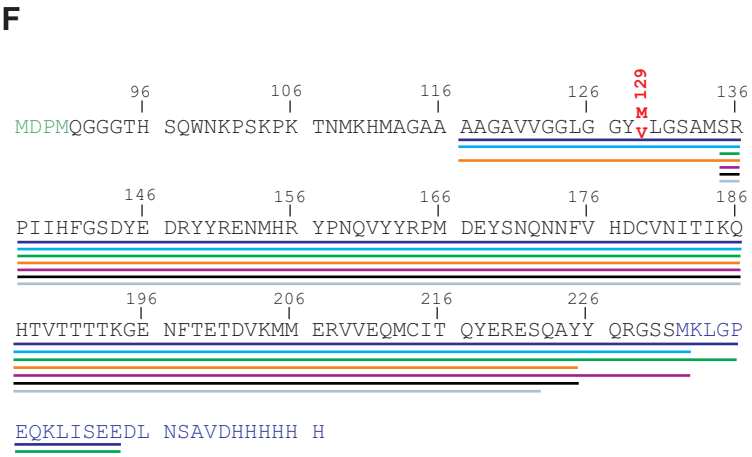

Figure 6
Tahiri-Alaoui et al.

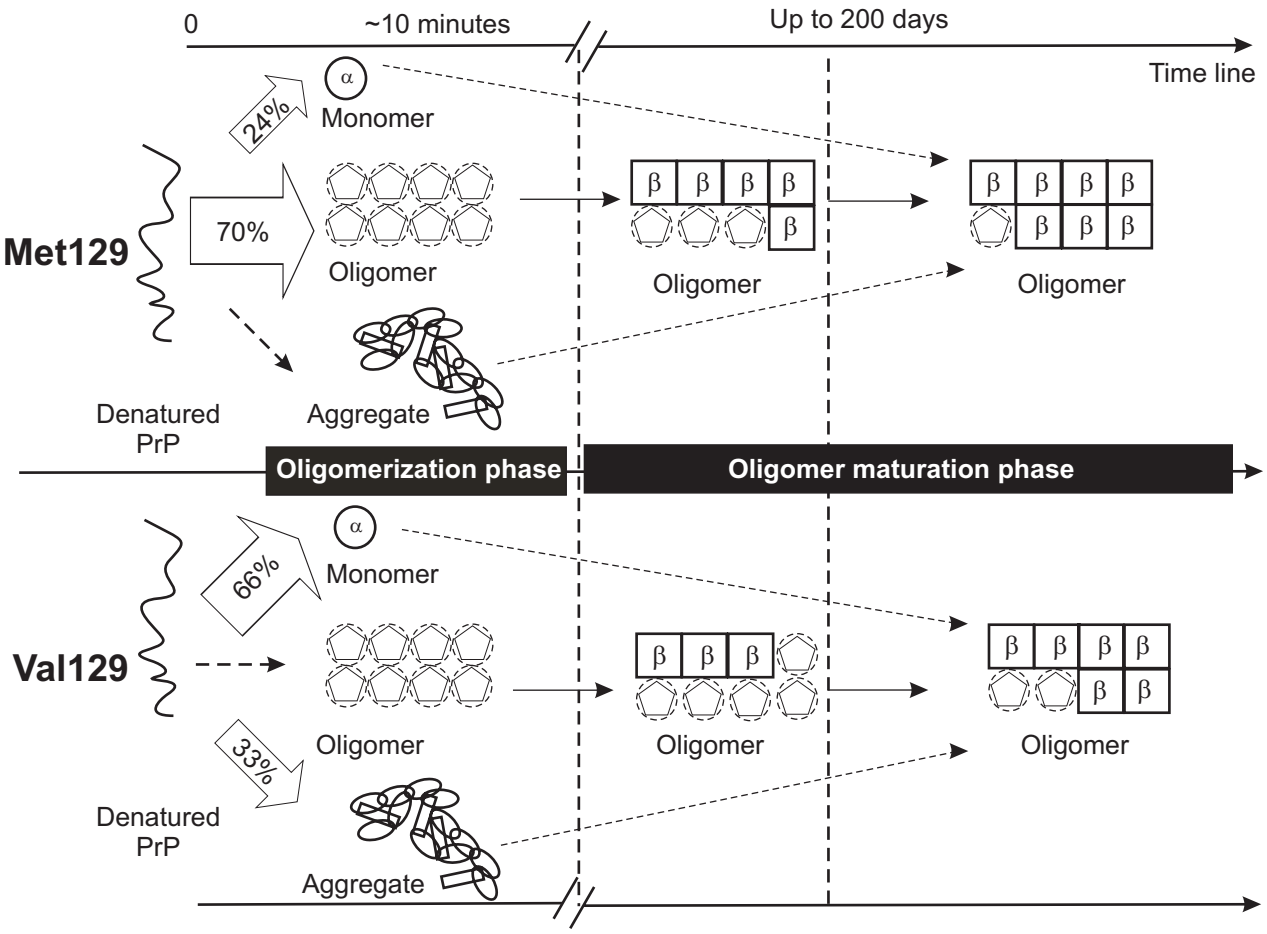

Supplementary Fig. 1 tahiri-alaoui et al.

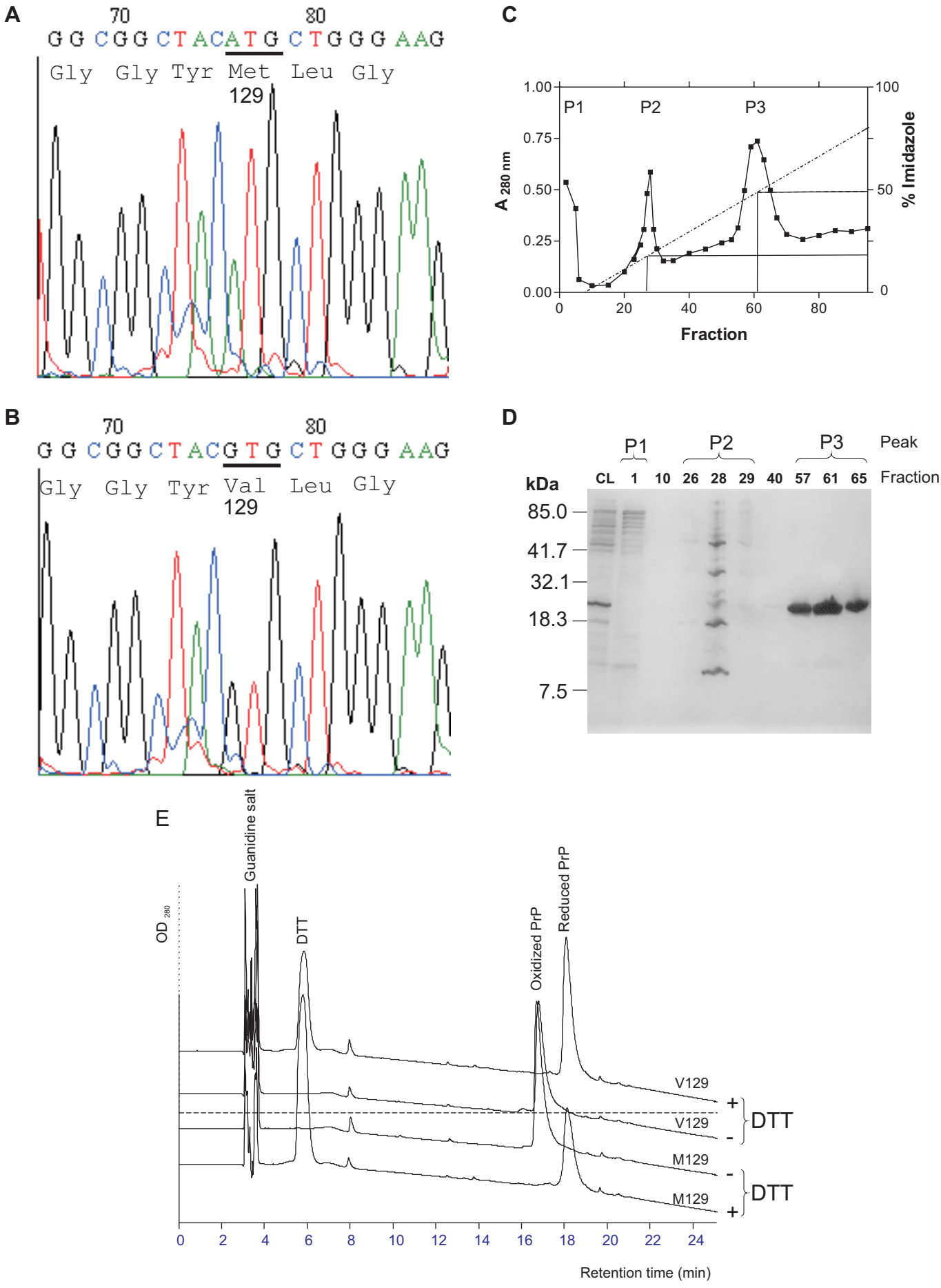

Supplementary Fig. 2 Tahiri-alaoui et

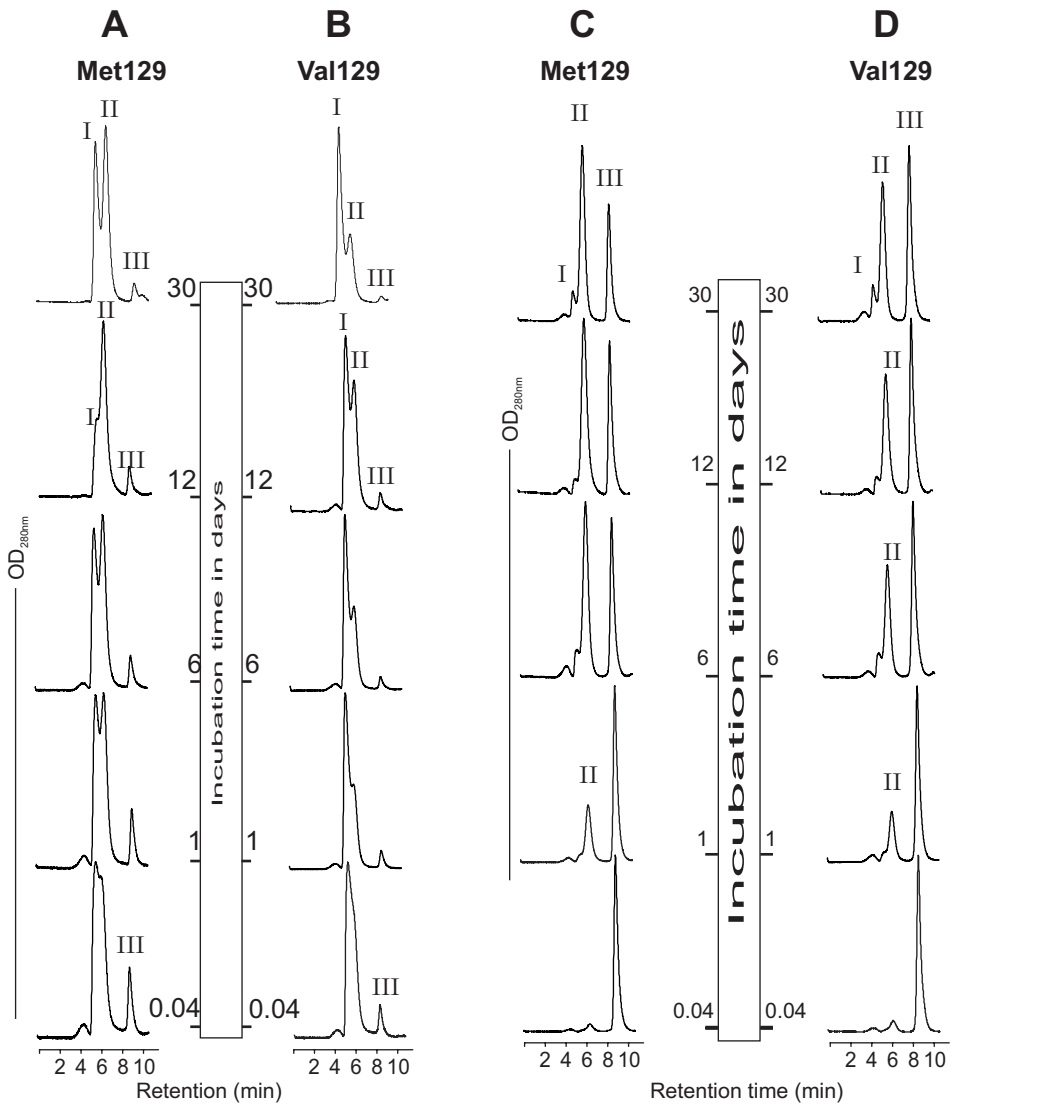

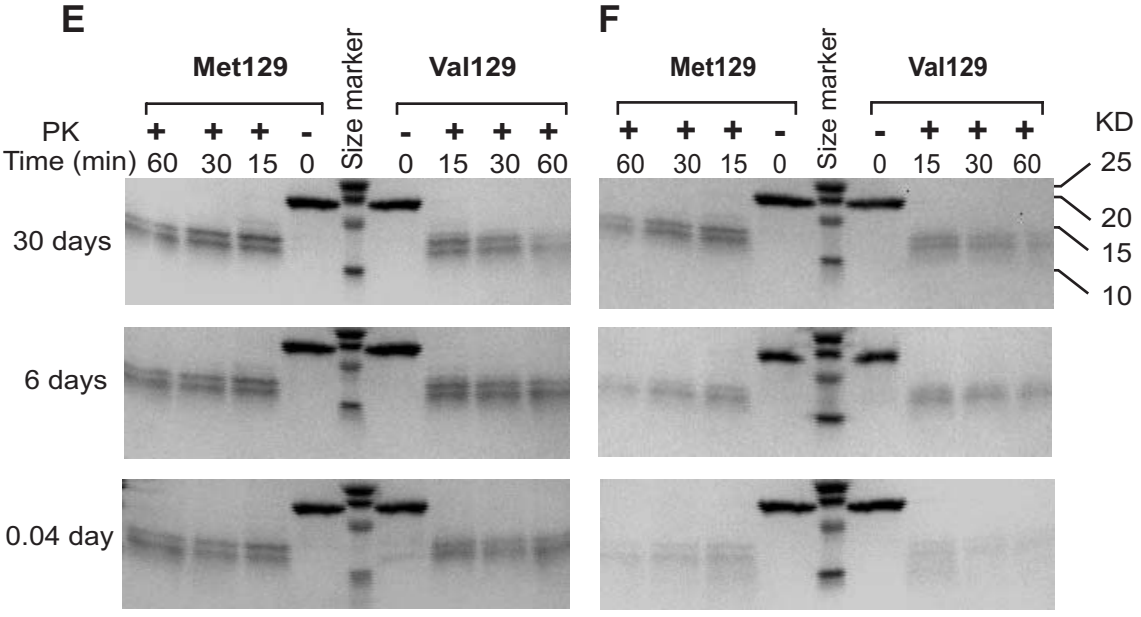

Supplementary Fig. 3 tahiri-Alaoui et al.

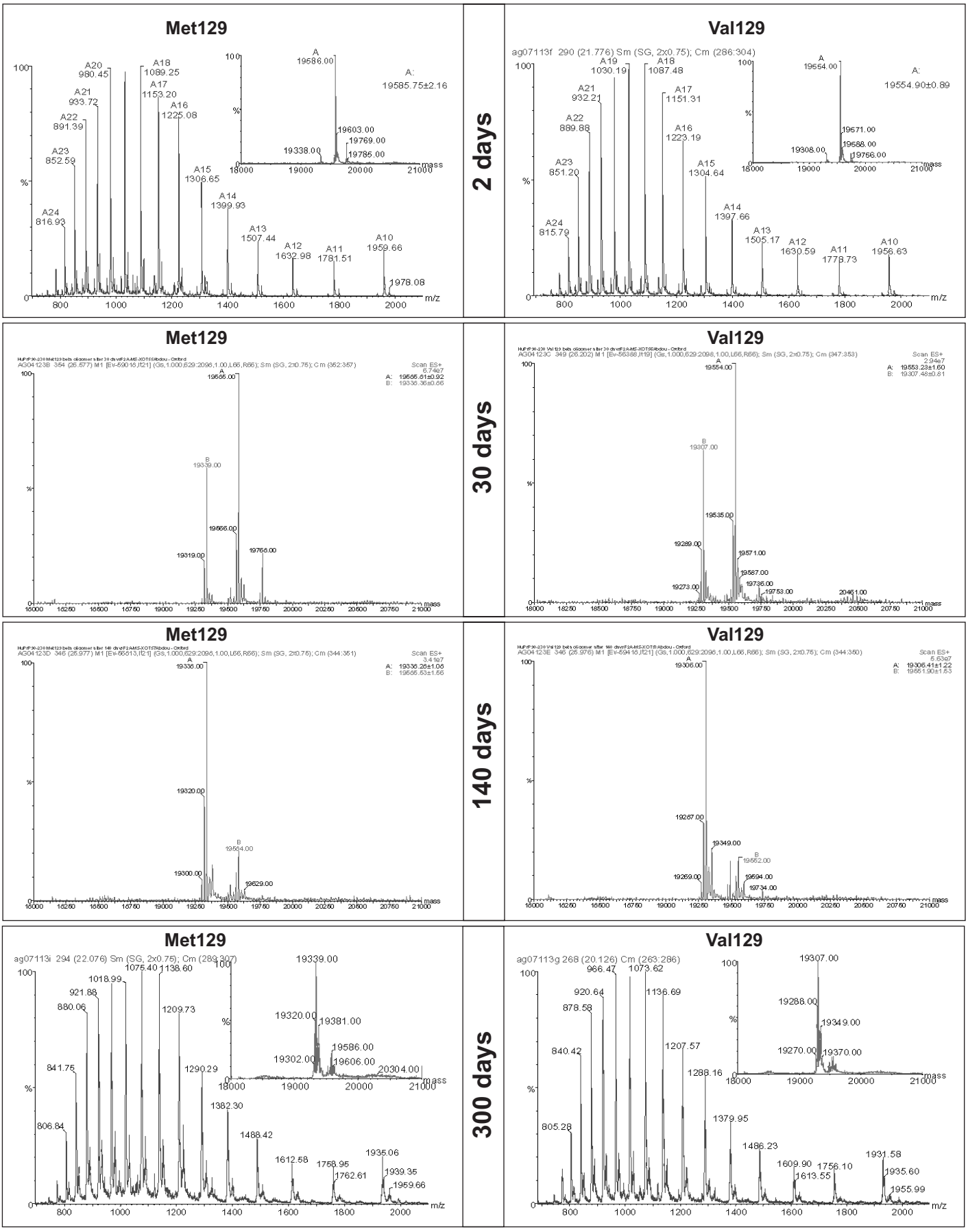

Supplementary Fig. 4 Tahiri-Alaoui et al.